PAPER

Unsupervised Speckle Level Estimation of SAR Images Using Texture Analysis and AR Model

Bin XU[†a)], **Yi CUI**[††], **Guangyi ZHOU**[†], **Biao YOU**[†], ***Nonmembers***, **Jian YANG**[†], ***Member***, ***and*** **Jianshe SONG**[†††], ***Nonmember***

SUMMARY In this paper, a new method is proposed for unsupervised speckle level estimation in synthetic aperture radar (SAR) images. It is assumed that fully developed speckle intensity has a Gamma distribution. Based on this assumption, estimation of the equivalent number of looks (ENL) is transformed into noise variance estimation in the logarithmic SAR image domain. In order to improve estimation accuracy, texture analysis is also applied to exclude areas where speckle is not fully developed (e.g., urban areas). Finally, the noise variance is estimated by a 2-dimensional autoregressive (AR) model. The effectiveness of the proposed method is verified with several SAR images from different SAR systems and simulated images.

key words: *AR model, equivalent number of looks (ENL), synthetic aperture radar (SAR), texture analysis.*

1. Introduction

Speckle originated from coherent imaging is a typical effect in synthetic aperture radar (SAR) images. For multilook processed SAR images [1], the speckle level is commonly characterized by the equivalent number of looks (ENL). Accurate estimation of the ENL plays an important role in many applications of SAR image processing. The ENL is a key input parameter that affects the despeckling performances for many classical and state-of-the-art filters [2]–[5]. In addition, it is an important evaluating indicator for SAR image despeckling [6], [7], and it is also very useful for target/edge detection [8], image classification [9], interferogram estimation [10] and so on. Since all these applications are very important in SAR and polarimetric SAR image processing, it is very urgent to estimate the ENL accurately.

By the definition of the ENL, a homogeneous area where speckle is fully developed must be selected for supervised estimation of the ENL. A well-trained human can easily identify a homogeneous area, but an automatic processing chain is surely preferable in many applications. There are several unsupervised methods. The methods proposed by Lee *et al*. [11], [12] draw a scatter plot of the mean versus standard deviation for each pixel within a sliding window. The Hough transform or angular sweep method is then used to estimate the ENL. The methods in [13] and [14] calculate the local ENL using a moving window over the SAR image. Then the ENL is estimated as the mode of the local ENL histogram. The method proposed by Cui *et al*. [15] establishes a lookup table between the ENL and the noise variance in the logarithmic SAR image, where the noise variance is estimated using a high-pass filter with image downsampling.

In this paper, we propose a new method for unsupervised speckle level estimation of SAR images. This method also transforms ENL estimation to noise variance estimation in the log-intensity SAR data [15]. However, two modifications are proposed to improve the estimation accuracy. First, the textural information in the SAR image is analyzed and flat regions are automatically chosen to estimate the speckle level. Second, the autoregressive (AR) model instead of high-pass filtering and downsampling is adopted to estimate the variance of the additive noise in the logarithmic SAR image.

The rest of the paper is organized as follows. Section 2 introduces the preparatory work including the logarithmic SAR image statistics and additive noise model. Noise variance estimation using texture analysis and AR model is presented in Section 3. Section 4 presents several results to discuss the improvement and the time complexity of the proposed method. Finally, Section 5 concludes this paper.

2. Logarithmic SAR Image Statistics and Additive Noise Model

In this section, we introduce the logarithmic SAR image statistics and the additive noise model of the logarithmic SAR image.

2.1 Logarithmic SAR Image Statistics

It is well established that the speckle in SAR images can be described by the following multiplicative noise model [1],

$$I_{i,j} = R_{i,j} \cdot n_{i,j}, \tag{1}$$

where $I_{i,j}$ denotes the observed intensity at a pixel (i, j); $R_{i,j}$ denotes the underlying target backscattering coefficient; $n_{i,j}$ denotes the multiplicative noise. For convenience, we only take intensity image into consideration in this study. If the speckle of the SAR image is fully developed, $n_{i,j}$ can be assumed to be a unit mean random variable of Gamma distribution parameterized by the ENL [1],

Manuscript received January 1, 2013.
Manuscript revised January 1, 2013.

[†]The authors are with the Department of Electronic Engineering, Tsinghua University, Beijing 100084, China.
[††]The author is with the Faculty of Engineering, Niigata University, Niigata 950-2181, Japan.
[†††]The author is with Xian Research Institute of Hi-Technology, Xian 710025, China.
a) E-mail: xubin07161@gmail.com
DOI: 10.1587/transcom.E0.B.1

$$p_n(n) = \frac{(\mathrm{ENL})^{\mathrm{ENL}} n^{\mathrm{ENL}-1}}{\Gamma(\mathrm{ENL})} e^{-n\mathrm{ENL}},\ n \geq 0, \tag{2}$$

where $\Gamma()$ is the Gamma function. In general, the ENL of a homogeneous region can be calculated by

$$\mathrm{ENL} = \frac{(\mathrm{mean})^2}{\mathrm{variance}}. \tag{3}$$

According to [16], the mean and variance of the logarithm of the multiplicative noise are

$$E[\ln(n)] = \psi^{(0)}(\mathrm{ENL}) - \ln(\mathrm{ENL}), \tag{4}$$

$$\mathrm{var}[\ln(n)] = \psi^{(1)}(\mathrm{ENL}), \tag{5}$$

respectively. Here $\psi^{(m)}(\mathrm{ENL})$ is the polygamma function of order m.

Equation (5) indicates that there is one-to-one relationship between $\mathrm{var}[\ln(n)]$ and the ENL. If $\mathrm{var}[\ln(n)]$ is obtained, the ENL can be solved numerically. Consequently, estimation of the speckle noise level, i.e., the ENL, can be equivalently transformed to estimation of the noise variance in the logarithmic domain, which will be the focus of this paper hereafter.

2.2 Additive Noise Model

By logarithmic transformation of (1), the multiplicative noise becomes additive, i.e.,

$$u_{i,j} = s_{i,j} + v_{i,j}, \tag{6}$$

where

$$u_{i,j} = \ln\left(I_{i,j}\right), \tag{7}$$

$$s_{i,j} = \ln\left(R_{i,j}\right) + \psi^{(0)}(\mathrm{ENL}) - \ln(\mathrm{ENL}), \tag{8}$$

$$v_{i,j} = \ln\left(n_{i,j}\right) - \psi^{(0)}(\mathrm{ENL}) + \ln(\mathrm{ENL}). \tag{9}$$

By (4), $v_{i,j}$ is a zero-mean additive noise. So the autocorrelation function (ACF) of $u(i, j)$ at coordinate (0,0) can be estimated by

$$r_{0,0} = E\left[u^2\right]. \tag{10}$$

Similarly, the ACF of $s(i, j)$ at coordinate (0,0) is

$$\bar{r}_{0,0} = E\left[s^2\right]. \tag{11}$$

Because s and v are independent stochastic processes, the variance of the additive noise is

$$\begin{aligned}\mathrm{var}(v) &= E\left[u^2\right] - E\left[s^2\right] - E[v]^2 \\ &= r_{0,0} - \bar{r}_{0,0}\end{aligned}. \tag{12}$$

Since $r_{0,0}$ can be easily obtained with the noisy process $u_{i,j}$, the remaining problem is the estimation of $\bar{r}_{0,0}$.

The basic idea to estimate $\bar{r}_{0,0}$ is that it can be interpolated by the adjacent ACF values of $u_{i,j}$ (see Fig.1). Thus from a broader perspective, the problem is closely related to ACF estimation (or spectral estimation, if in the view of frequency domain) for a stationary process. For such problems, the AR model is a very simple and effective method as is well established in the modern spectral estimation theory. Therefore, the estimation of $\bar{r}_{0,0}$ will be accomplished with the AR model in Section 3.2. However, since the noise $v_{i,j}$ is often spatially correlated [1], the ACF of $u_{i,j}$ within the effective range of noise ACF must be excluded. Fig.1 shows the 1-dimensional examples of the ACFs of v, u, and s, where A_x denotes the effective range of the noise ACF. A simple way to estimate the effective range of the noise ACF is stated in [15] where a high-pass filter $h_{i,j}$ is applied to the log-transformed SAR image $u_{i,j}$. Here $h_{i,j}$ is selected as the Laplace operator [17],

$$h = \begin{bmatrix} 1 & -2 & 1 \\ -2 & 4 & -2 \\ 1 & -2 & 1 \end{bmatrix}. \tag{13}$$

After high-pass filtering, the filtered image $w_{i,j}$ is mainly related to the noise process $v_{i,j}$ and can be approximated as

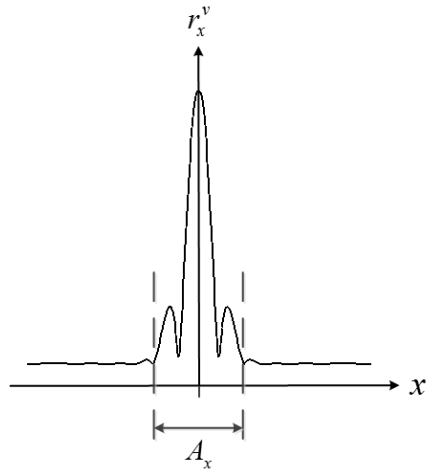

(a) The ACF of v along the x-axis.

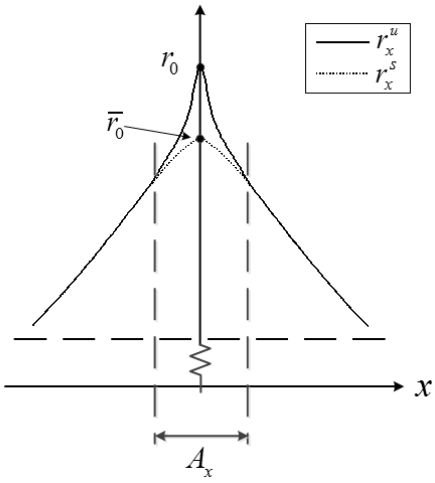

(b) The ACFs of u and s along the x-axis.

Fig. 1 The ACFs of v, u and s along the x-axis. A_x is the effective range of noise ACF along the x-axis.

[15],

$$w_{i,j} \approx v_{i,j} * h_{i,j}, \tag{14}$$

where "*" stands for the convolution operation.

Suppose that $r^v_{i,j}$ and $r^w_{i,j}$ are the ACFs of $v_{i,j}$ and $w_{i,j}$. Let l_x and l_y denote the lag lengths of $r^v_{i,j}$ along the x-axis and the y-axis respectively. If the effective range of $r^v_{i,j}$ is $(2l_x + 1) \times (2l_y + 1)$, then the effective range of $r^w_{i,j}$ becomes $(2l_x + 5) \times (2l_y + 5)$ [15]. Thus the effective range of the noise ACF can be deduced from the ACF of the high-pass filtered image. In order to improve the estimation accuracy, a 10 times interpolation by zero-padding fast Fourier transform or chirp z-transform is applied to $r^w_{i,j}$. To determine the effective range of $r^w_{i,j}$, we consider that the amplitude of $r^w_{i,j}$ larger than a predefined threshold (in percentage of $r^w_{0,0}$) is effective. Empirically, we find that 1% of the amplitude of $r^w_{0,0}$ is a proper choice since it produces an effective range with good trade-off of both sufficiently low noise ACF sidelobes and gap small enough to ensure the interpolation accuracy. For simplicity, only the main lobe and first sidelobe of $r^w_{i,j}$ are considered to estimate the effective range. In general, the boundary of the effective range forms an oval shape.

3. Noise Variance Estimation Using Texture Analysis and AR Model

3.1 Texture Analysis

Since the ENL is related to the Gamma distribution noise model which is only applicable for fully developed speckle, the presence of highly textured areas will cause significant ENL underestimation [11]–[15]. So such areas should be excluded for ENL estimation. The textural information is very rich in urban areas and poor in flat areas. Since textural features can be used for image classification [21]–[23], we analyze the textural information in SAR images and select flat regions where speckle is fully developed to estimate the speckle level.

The gray-level co-occurrence matrix (GLCM) is an effective tool for describing textural features. The elements in the GLCM represent the co-occurrence probabilities of the gray-levels and can be calculated by

$$p_{ij}(d, \theta) = \frac{S_{ij}}{\sum_{i,j=1}^{G} S_{ij}}, \tag{15}$$

where i and j are gray-levels; d denotes the interpixel distance; θ stands for the orientation angel between two pixels; G is the number of gray-levels and S_{ij} represents the number of occurrences of gray-levels i and j.

From the GLCM, 28 textural features can be derived [21]. The textural feature used in this study is entropy (ENT) which is defined as

$$ENT = -\sum_{i=1}^{G}\sum_{j=1}^{G} p_{ij} \ln p_{ij}. \tag{16}$$

In order to identify proper candidate areas, the image is divided into $K \times K$ non-overlapping blocks. For each block, the entropy is calculated by (15) and (16). It is expected that those blocks with the smallest entropy will be the least affected by texture. Therefore, we select the last several blocks with the lowest entropy as our candidate areas for ENL estimation. In practice, the percentage is fixed to the last 30% of all the blocks ranked by descending entropy. This choice was tested by using several SAR images and we found that it is effective. It is worth mentioning that the gray level of the SAR image should be quantized to 0~255 before texture analysis by GLCM. Although difference methods of quantization may change the absolute values of the calculated entropy for each block, their ranks will be invariant in general. Hence in this paper, the method proposed by Zhou *et al.* [25] is adopted for simple quantization.

3.2 AR Model

Now the remaining problem is the estimation of noise variance in the logarithmic SAR image for the $K \times K$ blocks selected by texture analysis. According to (12), we need to estimate $\bar{r}_{0,0}$ for each block.

In this paper, we use a 2-D AR model [18]–[20] to estimate $\bar{r}_{0,0}$. For each $K \times K$ block, the ACF is

$$r_{i,j} = E\left[u_{x,y} u_{x+i,y+j}\right]. \tag{17}$$

The size of the ACF is $N \times N$ where

$$N = 2K - 1. \tag{18}$$

As the ACF of the block is symmetrical, we use forward linear prediction to estimate $\bar{r}_{0,0}$. In the 2-D case, the forward linear predictor $\bar{r}_{i,j}$ is

$$\bar{r}_{i,j} = \sum_{m=0}^{p}\sum_{n=0}^{q} c_{m,n} r_{i-m,j-n}\ , \quad (m,n) \neq (0,0), \tag{19}$$

where $c_{m,n}$ are the linear predictor coefficients and (p, q) is the order of the 2-D AR model. It should be noted that the range of (i, j) is

$$S_1 = \{-N \leq i \leq N, -N \leq j \leq N\} \backslash A, \tag{20}$$

where A denotes the effective range of $r^v_{i,j}$ and "\" is the set difference.

In compact vector notation, (19) can be rewritten as

$$\bar{r}_{i,j} = \mathbf{r}^T_{i,j}\mathbf{c}, \tag{21}$$

where the superscript "^{T}" denotes the matrix transpose; $\mathbf{r}_{i,j}$ and $\mathbf{c}$ are listed in (22) and (23), respectively.

$$\mathbf{r}_{i,j} = \left[r_{i,j-1} \cdots r_{i,j-q}, r_{i-1,j} \cdots r_{i-1,j-q} \vdots \cdots \vdots r_{i-p,j} \cdots r_{i-p,j-q}\right]^T \tag{22}$$

$$\mathbf{c} = \left[c_{0,1} \cdots c_{0,q}, c_{1,0} \cdots c_{1,q} \vdots \cdots \vdots c_{p,0} \cdots c_{p,q}\right]^T \tag{23}$$

The forward linear prediction error $e_{i,j}$ is

$$e_{i,j} = r_{i,j} - \mathbf{r}_{i,j}^T \mathbf{c}. \tag{24}$$

Because of (20), the range of (i, j) in (24) is

$$S_2 = \{(k,l)|p - N \le k \le N, q - N \le l \le N\} \backslash S_3, \tag{25}$$

where S_3 caused by the effective range of $r_{i,j}^w$ is

$$S_3 = \bigcup_{(i,j)\in A} \{(k,l)|i \le k \le p + i, j \le l \le q + j\}. \tag{26}$$

The forward linear prediction error vector is

$$\mathbf{e} = \mathbf{a} - \mathbf{R}\mathbf{c}, \tag{27}$$

where $\mathbf{e}$, $\mathbf{R}$ and $\mathbf{a}$ are

$$\mathbf{e} = (\cdots e_{i,j} \cdots)^T_{(i,j)\in S_2}, \tag{28}$$

$$\mathbf{R} = (\cdots \mathbf{r}_{i,j} \cdots)^T_{(i,j)\in S_2}, \tag{29}$$

$$\mathbf{a} = (\cdots r_{i,j} \cdots)^T_{(i,j)\in S_2}. \tag{30}$$

Now the problem is to minimize $\mathbf{e^T e}$. The optimal solution of the linear predictor coefficients is

$$\mathbf{c} = (\mathbf{R}^T\mathbf{R})^{-1}\mathbf{R}^T\mathbf{a}. \tag{31}$$

With the linear predictor coefficients, $\bar{r}_{0,0}$ can be easily obtained. For example, if A is {(-1,0), (0,0), (1,0), (0,-1), (0,1)}, then $\bar{r}_{-1,0}$, $\bar{r}_{0,-1}$, and $\bar{r}_{0,0}$ can be obtained in turn as follows

$$\bar{r}_{-1,0} = \mathbf{r}_{-1,0}^T \mathbf{c}, \tag{32}$$

$$\bar{r}_{0,-1} = \mathbf{r}_{0,-1}^T \mathbf{c}, \tag{33}$$

$$\bar{r}_{0,0} = \mathbf{r}_{0,0}^T \mathbf{c} + a_{0,1}(\bar{r}_{0,-1} - r_{0,-1}) + a_{1,0}(\bar{r}_{-1,0} - r_{-1,0}). \tag{34}$$

After the noise variance is estimated for each $K \times K$ block, the mean of the results is regarded as the final estimate of the noise variance in the logarithmic SAR image. Then the ENL can be solved by numerical methods.

4. Experimental Results

4.1 Experimental Data

In Fig.2, ten SAR images from several different SAR systems are used to test the performance of the proposed method. The detailed information including sensor name, polarization and imaging area can be found in Table 1.

In order to further illustrate the advantages of using the AR model for ENL estimation, the proposed method is also tested on 1000 simulated SAR images. Each image contains a 128×128 homogeneous area contaminated by 4-look Gamma noises.

4.2 Results and Discussion

The unsupervised speckle level estimation algorithm is summarized in Fig.3, where several additional parameters are set as follows. First, as the specific choices of G and (d, θ) in (15) only affect the absolute values of ENT of each block but less likely their relative ranking, the influence of these two parameters on the result of texture analysis is insignificant. For simplicity, we set $(d, \theta) = (1, 0)$ and $G = 20$ which is pointed out by Ulaby *et al.* [23] as a good choice for SAR image classification. Also in consideration of both computational efficiency and estimation accuracy, the SAR image is empirically divided into 31×31 non-overlapping blocks and an AR model of $(p, q) = (5, 5)$ is applied for noise variance estimation.

Table 1 The detailed information of the test SAR images.

No.	Sensor name	Polarization	Imaging area
1	AIRSAR	VV	San Francisco, USA
2	AIRSAR	VV	Sydney, AUS
3	Convair	HH	Ice Area, CAN
4	Convair	HH	Ottawa, CAN
5	PISAR	HH	Tsukuba, JPN
6	SIR-C	VV	Tienshan, CHN
7	PALSAR	HH	Beijing, CHN
8	RADARSAT-2	HH	Dalian, CHN
9	TerraSAR-X	HH	Dalian, CHN
10	TerraSAR-X	HH	Dalian, CHN

As a first step, the effective range of $r_{i,j}^w$ can be estimated by the method described in Section 2.2. For example, $r_{i,j}^w$ of AIRSAR image of San Francisco (see Fig.2(a)) is shown in Fig.4(a) and the effective range of $r_{i,j}^w$ is the black region as shown in Fig.4(b). From the relationship between the effective range of $r_{i,j}^w$ and the effective range of $r_{i,j}^w$, we can obtain that A is {(-1,0), (0,0), (1,0), (0,-1), (0,1)}. Similar results have been also obtained for other SAR images.

In this study, the ENL estimation results of the proposed method are compared with two other unsupervised ENL estimation algorithms. One is that proposed by Cui *et al.* [15] which estimates the noise variance of the logarithmic image using a high-pass filter (HPF) and image downsampling. The other one is that proposed by Foucher *et al.* [13] which calculates the ENL in a small moving window over the whole image and uses the kernel density estimation (KDE) to choose the mode of the distribution as the final estimated ENL. In addition, the ENL is also estimated by supervised method [1], i.e., calculating the $(\text{mean})^2/\text{variance}$ of a homogeneous region which is selected manually and marked by the white rectangles in Fig.2. In this paper, this supervised ENL estimation is taken as the reference value for evaluation of unsupervised algorithms (although it may not necessarily represent the true ENL). Table 2 shows the nominal number of looks (NNL) and the ENL results estimated by the supervised method, the proposed method, the proposed method without texture analysis, the high-pass filter based method (Method 1) [15] and the local window and KDE based method (Method 2) [13].

Method 2 relies on the assumption that most of the regions in the SAR image are homogeneous. However, this assumption does not necessarily hold in richly textured terrain such as urban areas since SAR images of urban areas are known to be highly heterogeneous and can be described

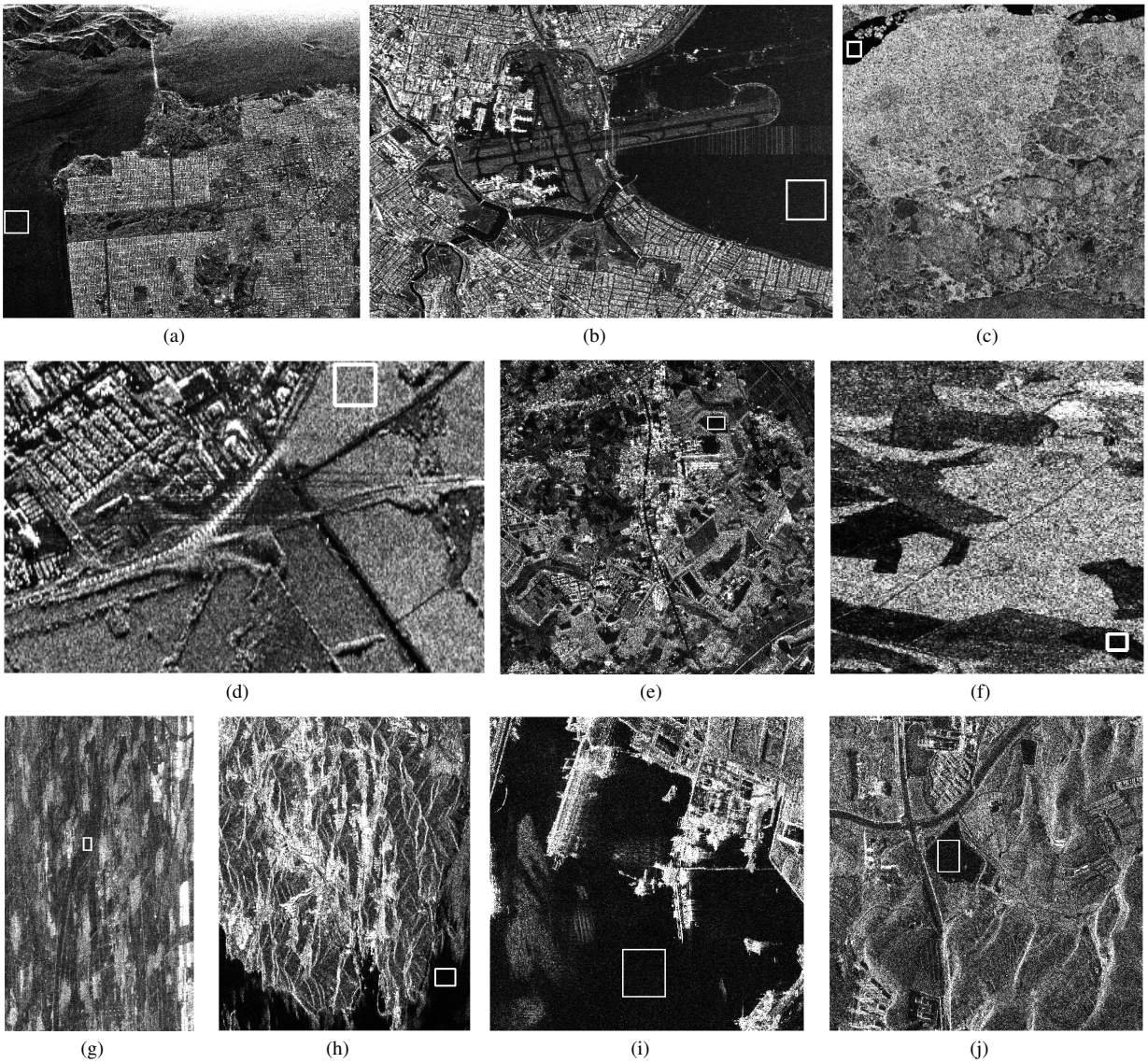

Fig. 2 Ten SAR images used to test the performance of the proposed method.

Input: SAR image(intensity image)
Step:
1. Texture analysis
a) SAR image gray-level quantization by [25].
b) Divide the quantized image into $K \times K$ non-overlapping blocks.
c) Calculate the GLCM and entropy by (15) and (16).
d) Select 30% of the blocks corresponding to smaller entropy for subsequent noise estimation.
2. Logarithmic transformation of the original (unquantized) SAR image
3. Noise estimation in the logarithmic SAR image
a) In the logarithmic SAR image, calculate the ACF of each block obtained by texture analysis.
b) For each block, calculate **R** and **a** by (22), (25), (29) and (30), and compute the linear predictor coefficients by (31). Then $\bar{r}_{0,0}$ can be easily obtained.
c) For each block, estimate the noise variance by (12). The mean of the estimation results is considered as the final estimation of the noise variance.
4. Estimation of the speckle level with the noise variance by numerical methods
Output: The ENL

Fig. 3 Unsupervised speckle level estimation algorithm proposed in this study.

by the Fisher distribution [26], [27]. It can be seen from Table 2 that this method underestimates the ENL for most of the test SAR images especially for those images where the assumption does not hold. On the other hand, the proposed method and Method 1 show better results.

Essentially, the proposed method and Method 1 both

Table 2 ENL estimation results. Method 1 is based on HPF with 2-fold down-sampling [15], and method 2 is based on the KDE with a 11×11 window [13]. The supervised estimation results and the best unsupervised estimation results are shown in bold.

No.	NNL*	Supervised method	Proposed	Proposed (Without texture analysis)**	Method 1 (HPF)	Method 2 (KDE)
1	4	**2.89**	3.21	**2.70**	2.48	0.95
2	18	**8.19**	**8.60**	4.18	2.91	0.33
3	10	**5.40**	**5.07**	4.57	4.14	3.03
4	10	**4.89**	**4.88**	4.06	2.28	0.27
5	4	**1.84**	**1.46**	1.36	1.37	1.00
6	4	**2.58**	2.46	**2.49**	2.42	2.04
7	6	**4.72**	**4.43**	4.08	4.12	2.89
8	4	**2.51**	**2.54**	2.09	2.10	0.71
9	1	**0.98**	1.04	1.03	1.00	**0.98**
10	1	**0.99**	1.04	1.02	**0.99**	0.89

* The NNL is the multiplication of the processing looks in the range and azimuth direction.
** In this case, all of the blocks are selected and textural information is not analyzed.

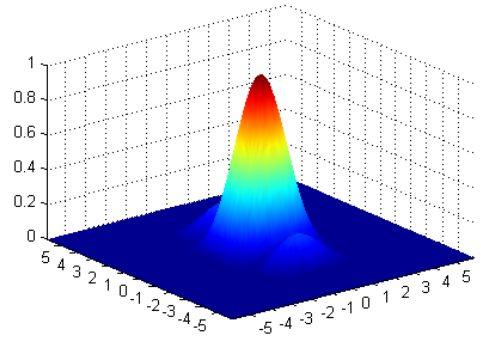

(a) $r^{w}_{i,j}$ of AIRSAR image of San Francisco (see Fig.2(a)).

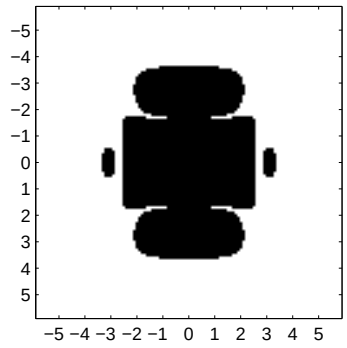

(b) The effective range of $r^{w}_{i,j}$.

Fig. 4 $r^{w}_{i,j}$ and its effective range of AIRSAR image of San Francisco (see Fig.2(a)).

estimate the noise variance in the logarithmic SAR image. However, Method 1 relies on the condition that the speckle of the whole image is fully developed whereas the proposed method pre-selects flat areas and so only requires that the speckle in these least textured regions is fully developed. Hence when the image has a lot of rich texture regions such as urban regions, the proposed method is expected to produce a much better result than Method 1. It can be seen in Table 2 that the proposed method performs similarly to

Table 3 The mean and variance of the ENL results of simulated images.

	Supervised method	Proposed (Without texture analysis)	Method 1 (HPF)
mean	**3.9986**	3.9985	3.9951
variance	0.0025	**0.0021**	0.0063

Method 1 for the two single-look test images but gives better results than Method 1 for the other multi-look images, especially for the second and the fourth test images. This is because both the latter two images are largely covered by urban areas where the speckle is not fully developed. The proposed method analyzes the textural information to exclude the urban area for ENL estimation which consequently leads to improved results. In addition, the proposed method also performs better than the same approach but without texture analysis (see the 4th and 5th column of Table 2). Clearly, the inclusion of texture analysis turns out to be an indispensable step for reliable ENL estimation.

Now we consider the effect of the AR model on ENL estimation. It can be seen from Table 2 that the proposed method even without texture analysis gives better results than Method 1 for the first four images and produces similar results to Method 1 for the other six images. Thus the superiority of AR model can be seen. To further confirm this superiority, we use 1000 simulated images as described in Section 4.1. Table 3 shows the mean and variance of the ENL results estimated by the supervised method, the proposed method without texture analysis and Method 1. From Table 3, one can see that using AR model to estimate the ENL can achieve a similar mean to those obtained by the supervised method and Method 1. However, the variance of the ENL results estimated by AR model is much closer to that obtained by the supervised estimation than that using a high-pass filter. With these results from real SAR images and simulated images, we can conclude that AR model is a more accuracy approach for ENL estimation.

Although the time complexity of the proposed method is higher than Method 1, the time complexity of the proposed method is still acceptable. Table 4 gives the computation time of the test SAR images. The proposed method was running on Matlab platform and the PC used to run this

Table 4 The computation time of the test SAR images by the proposed method.

No.	Image size	Computation time
1	900×1024	2.01s
2	601×889	1.05s
3	544×523	0.56s
4	222×342	0.21s
5	1000×1000	1.91s
6	256×256	0.15s
7	666×400	0.53s
8	500×400	0.44s
9	1000×1000	2.01s
10	1200×1200	2.81s

method had an Intel Core i5 processor with 2.80-GHz main frequency and 4.00-GB main memory. In general, the computation time is proportional to the image size and processing a 1000×1000 image typically takes around 2 seconds.

It should be noted that the estimation of the ENL is affected by the polarization and different polarizations lead to different estimation results. The polarimetric information can be jointly exploited to improve the ENL estimation accuracy. Anfinsen *et al.* [14] extended the definition of the ENL to the polarimetric SAR data based on the complex Wishart distribution. Thus the proposed method can also be extended to multi-polarization SAR data and we will focus on this point in future.

5. Conclusion

In this paper, an unsupervised method for speckle level estimation of SAR images has been proposed. The logarithmic SAR image statistics were adopted to transform the ENL estimation into the noise variance problem. Then we used texture analysis to avoid using rich textured areas (such as urban areas) where speckle is not fully developed. Finally, we applied a 2-D AR model for the noise variance estimation.

The proposed method was validated with real SAR images from different systems and simulated images. Experimental results showed that the combined approach of texture analysis and AR model can effectively improve the accuracy of unsupervised ENL estimation. In addition, the computational time of the proposed method was also found acceptable for practical applications.

6. Acknowledgment

The work was in part supported by the NSFC (No. 41171317), in part supported by the key project of the NSFC (No. 61132008) and in part supported by the Research Foundation of Tsinghua University. The authors would like to thank C. Liu and Z. Li for the helpful discussions on the AR model and also the reviewers for their constructive comments.

References

[1] C. Oliver, S. Quegan, Understanding synthetic aperture radar images with CDROM, 2nd ed. Raleigh, NC: SciTech, 2004.
[2] J.S. Lee, "Digital image enhancement and noise filtering by use of local statistics," IEEE Trans. Pattern Anal. Mach. Intell., vol. PAMI-2, no. 2, pp. 165-168, Mar. 1980.
[3] J.S. Lee, J.H. Wen, T.L. Ainsworth, K.S. Chen, A.J. Chen, "Improved sigma filter for speckle filtering of SAR imagery," IEEE Trans. Geosci. Remote Sens., vol. 47, no. 1, pp. 202-213, Jan. 2009.
[4] S. Parrilli, M. Poderico, C.V. Angelino, L. Verdoliva, "A nonlocal SAR image denoising algorithm based on LLMMSE wavelet shrinkage," IEEE Trans. Geosci. Remote Sens., vol. 50, no. 2, pp. 606-616, Feb. 2012.
[5] H. Woo, S. Yun, "Alternating minimization algorithm for speckle reduction with a shifting technique," IEEE Transactions on Image Processing, vol. 21, no.4, pp. 1701-1714, April 2012.
[6] W.G. Zhang, Q. Zhang, C.S. Yang, "Improved bilateral filtering for SAR image despeckling," Electronics letters, vol. 47, no. 4, pp. 286-288, Feb. 2011.
[7] D.E. Molina, D. Gleich, M. Datcu, "Gibbs random field models for model-based despeckling of SAR images," IEEE Geosci. Remote Sens. Letters, vol. 7, no. 1, pp. 73-77, Jan. 2010.
[8] R. Touzi, A. Lopes, P. Bousquet, "A statistical and geometrical edge detector for SAR images," IEEE Trans. Geosci. Remote Sens., vol. 26, pp. 764-773, Nov. 1988.
[9] H. Skriver, "Crop Classification by Multitemporal C-and L-Band Single-and Dual-Polarization and Fully Polarimetric SAR," IEEE Trans. Geosci. Remote Sens., vol. 50, no. 6, pp. 2138-2149, June 2012.
[10] C.A. Deledalle, L. Denis, F. Tupin, "NL-InSAR: Nonlocal interferogram estimation," IEEE Trans. Geosci. Remote Sens., vol. 49, no. 4, pp. 1441-1452, April 2011.
[11] J.S. Lee, and K. Hoppel, "Noise modeling and estimation of remotely-sensed images," in Proc. IEEE IGARSS, Vancouver, BC, Canada, vol. 2, pp. 1005-1008, July 1989.
[12] J.S. Lee, K. Hoppel, and S.A. Mango, "Unsupervised estimation of speckle noise in radar images," Int. J. Imaging Syst. Technol., vol. 4, no. 4, pp. 298-305, 1992.
[13] S. Foucher, J.M. Boucher, and G.B. Benie, "Maximum likelihood estimation of the number of looks in SAR images," in Proc. Int. Conf. Microw., Radar Wireless Commun., Wroclaw, Poland, vol. 2, pp. 657-660, 2000.
[14] S.N. Anfinsen, A.P. Doulgeris, T. Eltoft, "Estimation of the equivalent number of looks in polarimetric synthetic aperture radar imagery," IEEE Trans. Geosci. Remote Sens., vol. 47, no. 11, pp. 3795-3809, Nov. 2009.
[15] Y. Cui, G. Zhou, J. Yang, and Y. Yamaguchi, "Unsupervised estimation of the equivalent number of looks in SAR images," IEEE Geosci. Remote Sens. Letters, vol. 8, no. 4, pp. 710-714, July 2011.
[16] D.H. Hoekman, "Speckle ensemble statistics of logarithmically scaled data," IEEE Trans. Geosci. Remote Sens., vol. 29, no. 1, pp. 180-182, Jan. 1991.
[17] J. Immerkaer, "Fast noise variance estimation," Computer Vision and Image Understanding, vol. 64, no. 2, pp. 300-302, 1996.
[18] K.S. Sim, S.K. Nidal, "Image signal-to-noise ratio estimation using the autoregressive model," Scanning, vol. 26, pp. 135-139, 2004.
[19] J.A. Cadzow and K. Ogino, "Two-dimensional spectral estimation," IEEE Trans. Acoust., Speech, Signal Processing, vol. ASSP-29, pp. 396-401, June 1981.
[20] B. Aksasse, and L. Radouane, "Two-dimensional autoregressive (2-D AR) model order estimation," IEEE Trans. Signal Processing, vol. 47, no. 7, pp. 2072-2077, July 1999.
[21] R.M. Haralick, K. Shanmugan, and I. Dinstein, "Textural features for image classification," IEEE Transactions on Systems, Man, and Cybernetics, Vol. SMC-3, no. 6, pp. 610-621, Nov. 1973.

[22] G. Zhou, Y. Cui, Y. Liu, and J. Yang, "A binary tree structured terrain classifier for Pol-SAR images," IEICE Transactions on Communications, vol. E94-B, no. 5, pp. 1515-1518, 2011.
[23] F.T. Ulaby, F. Kouyate, B. Brisco, T.H.L. Williams, "Texture information in SAR images," IEEE Trans. Geosci. Remote Sens., vol. GE-24, no. 2, pp. 235-245, March 1986.
[24] PALSAR algorithm description, Vexcel Corporation, 2003, pp. 68-69.
[25] G. Zhou, H. Zhong, J. Yang, "A novel method of visualization for SAR images," in Proc. Int. Conf. Intell. Computation Technology and Automation, vol. 2, pp. 373-376, 2011.
[26] L. Bombrun, J.M. Beaulieu, "Fisher distribution for texture modeling of polarimetric SAR data," IEEE Geosci. Remote Sens. Letters, vol. 5, no. 3, pp. 512-516, July 2008.
[27] L. Bombrun, G. Vasile, M. Gay, F. Totir, "Hierarchical segmentation of polarimetric SAR images using heterogeneous clutter models," IEEE Trans. Geosci. Remote Sens., vol. 49, no. 2, pp. 726-737, Feb. 2011.

Bin Xu received the B.S. degree from Tsinghua University, Beijing, China, in 2011, where he is currently working toward the Ph.D. degree in the Department of Electronic Engineering. His research work focuses on SAR image processing and polarimetric SAR image processing.

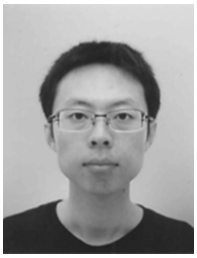

Yi Cui received the B.S. degree (with honors) in electronic information science and technology from Jilin University, Changchun, China, in 2006 and the Ph.D. degree in information and communication engineering from the Tsinghua University, Beijing, China, in 2011. From August 2011 to March 2013, he was a postdoctoral fellow with Niigata University (Japan) where he is now an assistant professor. His research interests include SAR image processing, radar polarimetry, and electromagnetic theory. Dr. Cui is the first-prize winner of the student paper competition at the 2010 Asia-Pacific Radio Science Conference (AP-RASC'10), and a recipient of the best paper award of the 2012 International Symposium on Antennas and Propagation (ISAP'2012).

Guangyi Zhou received the B.S. and Ph.D. degrees from Tsinghua University, Beijing, China, in 2006 and 2011, respectively. His research work focuses on polarimetric synthetic aperture radar image processing and polarimetric interferometric data processing.

Biao You received the B.S. and M.S. degree from Zhengzhou Information Science and Technology Institute, Henan, China, in 1996 and 2001, respectively. He is currently working toward the Ph.D. degree in the Department of Electronic Engineering. His research work focuses on polarimetric SAR image interpretation.

Jian Yang received the B.S. and M.S. degrees from Northwestern Polytechnical University, Xian, China, in 1985 and 1990, respectively, and the Ph.D. degree from Niigata University, Niigata, Japan, in 1999. In 1985, he was with the Department of Applied Mathematics, Northwestern Polytechnical University. From 1999 to 2000, he was an Assistant Professor with Niigata University. In April 2000, he was with the Department of Electronic Engineering, Tsinghua University, Beijing, China, where he is currently a Professor. His interests include radar polarimetry, remote sensing, mathematical modeling, optimization in engineering, and fuzzy theory. Dr. Yang is the Chairman of The Institute of Electronics, Information and Communication Engineers in Beijing area and the Vice-Chairman of the IEEE Aerospace and Electronic Systems in Beijing chapter.

Jianshe Song received the B.S. degree Shanxi Normal University in 1982, and received M.S. and Ph.D degrees from Xidian University in 1989 and 2001, respectively. He is now a professor of Xian Research Institute of Hi-Technology. He has finished many projects and received more than ten awards from Chinese government. He published five books and more than 150 papers. His interests include radar theory, signal processing and optimization in engineering.